Journal of Orthopaedic Translation 51 (2025) 278–289

Contents lists available at ScienceDirect

Journal of Orthopaedic Translation

journal homepage: www.journals.elsevier.com/journal-of-orthopaedic-translation

Original article

The role of Piezo1 in bone marrow stem cells in response to elevated intraosseous pressure on regulating osteogenesis and angiogenesis of steroid-induced osteonecrosis of the femoral head

Zilin Li [a,1], Lizhi Han [b,1], Bo Wang [c,1], Ping Wang [a], Yuxi Wang [a], Ruoyu Wang [a], Xiao Lv [a,**], Yong Feng [a,*]

[a] Department of Orthopedics, Union Hospital, Tongji Medical College, Huazhong University of Science and Technology, Wuhan, China
[b] Department of Orthopedics, The First Affiliated Hospital of Bengbu Medical University, Anhui Key Laboratory of Tissue Transformation, Bengbu Medical University, Bengbu, 233000, Anhui Province, China
[c] Department of Rehabilitation, Wuhan No. 1 Hospital, Tongji Medical College, Huazhong University of Science and Technology, Wuhan, China

ARTICLE INFO

Keywords:
Bone marrow stem cells
Elevated intraosseous pressure
Piezo1
Steroid-induced osteonecrosis of femoral head

ABSTRACT

Objectives: Steroid-induced osteonecrosis of the femoral head (SONFH) remains a significant global health issue, with an unclear pathogenesis. Elevated intraosseous pressure is considered a key initiating factor in SONFH development. Impaired osteogenesis and angiogenesis are believed to be critical in SONFH progression. Piezo1, a mechanosensitive cation channel, may sense changes in intraosseous pressure. In this study, we set out to explore the role of Piezo1 in SONFH and how to target Piezo1 to treat SONFH.

Methods: Femoral head tissue specimens were collected from patients with ONFH and femoral neck fracture. Histological staining, Western blotting, and RT-PCR analysis were conducted to investigate the relationship between elevated intraosseous pressure and SONFH in rat models. Immunofluorescence staining of femoral head tissues was performed to study the spatiotemporal relationship between elevated intraosseous pressure and angiogenesis, osteogenesis, and development of SONFH.

Results: In the early stages of SONFH, elevated intraosseous pressure increased angiogenesis and osteogenesis. However, as the pressure continued to rise, both processes were inhibited. Furthermore, Elevated intraosseous pressure activated the Piezo1 signaling pathway in bone marrow stem cells. Piezo1 activation led to increased intracellular calcium influx, thus enhancing osteogenesis and angiogenesis through CAM-NFAT1 signaling pathway.

Conclusion: In the early stages of SONFH, Piezo1 in BMSCs senses increased intraosseous pressure, promoting angiogenesis and osteogenesis. Targeting Piezo1 to promote the osteogenic and angiogenic potential of stem cells, which could curb further increases in pressure, contribute to early treatment of SONFH.

The translational potential of this article: Currently, many mechanisms of the impact of elevated intraosseous pressure on osteonecrosis of the femoral head are still in the basic theoretical research stage, and we hope to translate them into clinical applications as soon as possible. We discovered that targeting Piezo1 curb further increases in intraosseous pressure, alleviating the damaging effects of glucocorticoids on stem cells and blood vessels, which exerting great significance in treatment of early stage SONFH.

1. Introduction

Osteonecrosis of the femoral head (ONFH) is a refractory bone-destroying disease commonly occurring in patients following trauma or systemic glucocorticoid (GC) treatment [1]. The primary pathological feature is the progressive death of bone cell lines (mesenchymal stem cells, osteoblasts, osteocytes, etc.) and other bone marrow cells, eventually leading to structural changes or collapse of the femoral head and

* Corresponding author.
** Corresponding author.
E-mail addresses: lvxiaotjmu@163.com (X. Lv), fengyong@hust.edu.cn (Y. Feng).
[1] Zilin Li, Lizhi Han and Bo Wang contributed equally to the manuscript and should be considered co-first authors.

https://doi.org/10.1016/j.jot.2025.01.008
Received 8 September 2024; Received in revised form 18 December 2024; Accepted 8 January 2025

hip joint dysfunction [2–4]. In China, over 8 million cases of ONFH have been reported. Clinical studies indicate that the incidence rate of ONFH in the UK is 1.4 cases per 100,000 people, which is comparable to the 1.9 cases per 100,000 people reported in Japan [5]. Thus, early intervention in ONFH, prior to femoral head collapse, is crucial to delay or even avoid total hip replacement. Steroid-induced osteonecrosis of the femoral head (SONFH) is associated with increased intraosseous pressure caused by enhanced lipogenesis in the bone marrow, adipocyte hypertrophy, and local vascular dysfunction in the femoral head, resulting in reduced blood flow and ultimately leading to femoral head dysfunction [6–9]. Various treatment strategies are employed in the early clinical stages of SONFH, with core decompression (CD) being the most commonly used and showing significant efficacy [10–12]. However, further research is required to evaluate these methods and explore the mechanisms underlying successful stress reduction. This study focuses on the pattern of increased intraosseous pressure during ONFH progression, explores its phenotype and intrinsic mechanism in the SONFH, and seeks targeted regulation of intraosseous pressure to alleviate SONFH.

The Piezo1 protein, a mechanosensory cation channel complex discovered by Patapoutian, the 2021 Nobel Prize winner, plays a crucial role in bone homeostasis [15–19]. Under physiological conditions, Piezo1 in osteoblast cells maintains bone homeostasis by responding to mechanical stimulation [20,21]. It has been reported that Piezo1 acts as a lineage differentiation determinant in MSCs by regulating the expression of BMP2, thereby balancing their osteogenic and adipogenic differentiation [22,23]. Piezo1 promotes osteogenesis of mesenchymal stem cells, and bone formation by osteoblasts and osteocytes under mechanical stimulation, maintaining bone homeostasis [24–27]. Additionally, Piezo1 mediates mechanosensory-activated bone marrow macrophages to secrete VEGF-A, promoting sinusoid regeneration and hematopoietic reconstruction [28]. However, under pathological conditions, excessive activation of Piezo1 mediates an influx of Ca^{2+}, causing intracellular Ca^{2+} overload, thus leading to chondrocyte apoptosis and exacerbating arthritis progression [29]. Furthermore, Piezo1 in endothelial cells can mediate pressure-induced pulmonary vascular hyperpermeability by disrupting adherens junctions, contributing to the progression of pulmonary edema [30]. Mechanical stimulation also drives Piezo1 to mediate the Ca^{2+}/NF-κB pathway in nucleus pulposus cells, promoting the production of the NLRP3 inflammasome and leading to stress induced degeneration of these cells [31]. The role of Piezo1 in the progression of osteonecrosis of the femoral head, however, has yet to be elucidated.

Previous studies have shown that patients with ONFH exhibit high-signal changes of bone marrow edema on MRI in the early stages of the disease, though the presence of high-signal edema does not always lead to osteonecrosis [32–37]. While steroid-induced ONFH accounts for a significant proportion of cases, not all patients receiving high-dose glucocorticoid therapy develop osteonecrosis; the disease outcome can vary between necrosis and improvement [38–40]. Clinical studies suggest that intraosseous pressure and the course of osteonecrosis improve following stem cell transplantation and interventions to enhance blood supply to the femoral head in the early stages of the disease, which shed lights on the early treatment of ONFH [41–44]. This study found that Piezo1 on stem cells could respond to early increase in intraosseous pressure and promoted their osteogenic and angiogenic potential. Targeting stem cell Piezo1 may help regulate intraosseous pressure and achieve early prevention and treatment of SONFH.

2. Materials and methods

2.1. Experimental animals

The experimental animals used in this study were SD rats. Among them, suckling SD rats about 5 days old were used for primary cell collection, and 12-week-old SPF male SD rats were used for animal model experiments. All experimental animals were purchased from the Animal Experiment Center of Tongji Medical College, Huazhong University of Science and Technology. All animal experiments were approved by the Animal Ethics Committee of Tongji Medical College, Huazhong University of Science and Technology. All personnel involved in the experiments obtained the necessary qualifications.

2.2. Extraction of mRNA and real-time quantitative polymerase chain reaction

Total RNA was extracted using Trizol reagent according to the manufacture's instructions. RNA concentration and purity were measured using absorbance at 260 and 280 nm using a NanoDrop 2000 spectrophotometer (Thermo Fisher Scientific, Waltham, USA). The RNA was then reverse transcribed using PrimeScript RT regent Kit (TaKaRa). The levels of individual genes were measured by qPCR using SYBR Premix (TaKaRa, Japan) in a Bio-Rad CFX-96 system (Bio-Rad, USA). The reaction was carried out in triplicate. The levels of mouse Piezo1 were determined using the following primers: forward 5′-AGCTTGGAGCTGGATGATGACGATGATAGTGAAGCCACAGAT GTATCATCGTC ATCATCCAGCTCCC-3; reverse 5′-TCGAGGGAGCTGGATGAT GACGAT GATACATCTGTGGCTTCACTATCATCGTCATCATCCAGCTCCA-3. Relative gene expression was calculated using the relative standard curve method ($2-\Delta\Delta Ct$), and β-actin or GAPDH was used as a control for internal normalization.

2.3. Measurement of intramedullary pressure in rats

(1) Anesthetize SD rats with chloral hydrate (0.35 ml/100g, intraperitoneal injection), and fix them on the operating table in a supine position. Both hip joints are abducted and slightly flexed, and both knee joints are flexed approximately 30–45°. (2) Connect the tee tube to the pressure sensor, connect the measuring instrument, connect the outlet of the tee tube to the polyethylene catheter, and inject 0.5 ml of heparin saline into the tube through the tee tube to drain out the air bubbles. (3) Open the pressure measurement software and zero the initial pressure. During zero adjustment, the end of the polyethylene conduit should be kept level with the position during pressure measurement. (4) Use a lumbar puncture needle to puncture through the cortical bone approximately 0.5 cm above the medial femoral condyle, and then remove the needle core after entering 2.5 cm into the medullary cavity. (5) Insert the polyethylene catheter connected to the tee tube and the pressure sensor into the lumbar puncture needle with the needle core removed, and extend it to the needle tip, exposing 0.5 cm (6) For pressure measurement, the distance between the polyethylene catheter and the femoral pressure measurement part on both sides of the rat should be consistent. The catheter enters the medullary cavity for 2 min, that is, 1 min after the pressure at each site stabilizes, and record the pressure data.

2.4. Immunofluorescence analysis

For immunofluorescence staining, cells were placed on Matrigel-coated dishes and fixed with 4 % PFA for 10 min. Myofibers were fixed with 2 % PFA for 10 min. After permeabilization in 0.1 % Triton; 1:200), immunofluorescence signals were visualized with Alexa488-or Alexa594-conjugated secondary antibodies using a fluorescence microscope (AXIO Observer Z1, Zeiss) equipped with 63 × , 40 × , and 20 × objectives. Fluorescence intensity was quantified using ImageJ software for further statistical analysis. To detect EdU in immunostained samples, click chemistry reactions were performed after staining with primary and secondary antibodies using the Click-iT EdU Imaging Kit (Life Technologies) according to the manufacturer instructions.

2.5. Western blotting analysis

In this study, proteins were subjected to sodium dodecyl sulfate-polyacrylamide electrophoresis, transferred to polyvinylidene

difluoride membrane, and incubated with primary antibodies overnight. The membrane was then washed, incubated with secondary antibodies, and protein bands were visualized using enhanced chemiluminescence reagents.

2.6. Laminar shear stress

Laminar flow studies were conducted at 37 °C using a parallel plate flow system. Briefly, constant shear stress was applied by perfusing BMSCs with a continuous medium flow at 20 dyn/cm^2 cycles [45–47]. BMSCs under static conditions were used as controls.

2.7. Calcium influx measurement

Changes in intracellular Ca^{2+} levels were measured by the fluorescent Ca^{2+}-sensitive dye Fluo-4 AM (F14201, Invitrogen) according to published protocols. Cells were incubated with 5 μM Fluo-4 AM in HBSS-HEPES buffer without Ca^{2+} and Mg^{2+} for 30 min at 37 °C, and then the cells were washed three times with HBSS-HEPES buffer. Time-lapse images were collected every 1.5 s using a Leica SP8 MP microscope using an immersion 40 × objective. The excitation wavelength was set to 488 nm and emission was recorded at 535 ± 15 nm. Image sequences were analyzed and processed using ImageJ/FIJI software.

2.8. Experimental detection of EC migration and tube formation in vitro

To assess BMEC migration, 1 × 10^4 primary BMECs (approximately 150 μl medium) were seeded into the upper chamber of Transwell plates (8 μm wells; Corning, NY, USA) and incubated at 37 °C for 12 h. Migrated BMECs in the lower chamber were stained with 1 % crystal violet for 5 min, and the number of cells in 5 fields of each chamber was counted. For in vitro tube formation assays, 96-well plates were pre-coated with Matrigel (Corning, New York, USA). Then, primary BMECs (0.7 × 10^4 cells) were seeded into the wells, and images were captured after 6 h.

2.9. Data processing

All experiments in this topic were independently repeated three times or more, and the data are expressed as mean ± SEM. Prism software (GraphPad version 8.0) or SPSS software was used for data analysis and comparison. When conducting statistical analysis of data, the t test was used to compare data between two groups, and One-way ANOVA was used to analyze and compare data between multiple groups. Differences were considered statistically significant when the P value was less than 0.05.

3. Results

3.1. The intraosseous pressure continues to increase in the early to mid-stage of SONFH (SONFH2-6W), and the pressure decreases at the end stage (SONFH6-8W)

Previous studies have discovered elevated intraosseous pressure in both ONFH patients and animal models [1,11]. However, the progression of intraosseous pressure during osteonecrosis and its localized impact on the femoral head require further investigation. This study developed a steroid-induced femoral head rat model to measure intraosseous pressure changes. Rats were injected intraperitoneally with lipopolysaccharide (LPS, Sigma, USA) at 100 μg/kg daily for three consecutive days, followed by intramuscular injections of methylprednisolone (MPS, Pfizer Pharmaceuticals, China) at 100 mg/kg daily for three consecutive days [3,4]. One week later, injections continued for two days per week for four weeks (Fig. 1A). Specimens were collected at 2, 4, 6, and 8 weeks.

Hematoxylin and eosin (H&E) staining of specimens taken from animal models revealed severe damage to trabecular bone and bone marrow structures, with fat vacuoles and necrotic cells evident in MPS-treated rats. Empty osteocyte lacunae, indicative of osteonecrosis, were present in residual trabecular bone, whereas saline-treated control rats showed minimal osteonecrosis from SONFH4W to SONFH8W (Fig. 1B). Intraosseous pressure measurements (Table S1) indicated a continuous

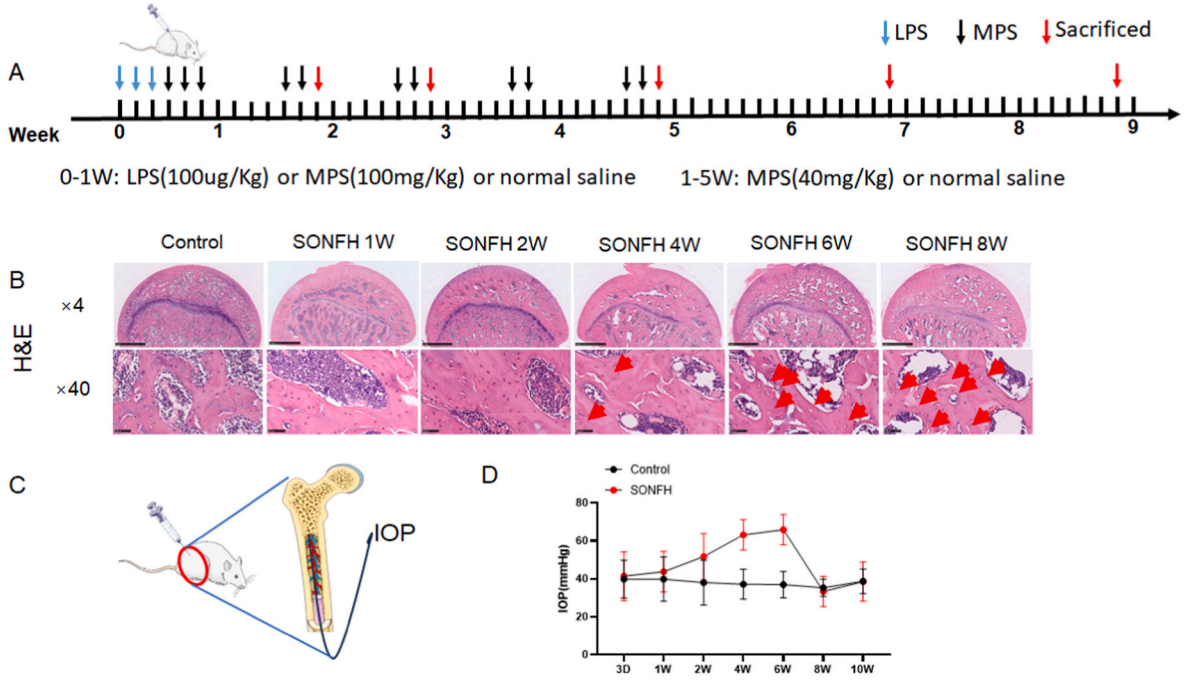

Fig. 1. Change in intraosseous pressure levels during the process of SONFH models. (A) Modeling scheme for steroid-induced femoral head necrosis in rats; LPS: lipopolysaccharide; MPS: methylprednisolone. (B) HE changes in rat femoral head tissue during ONFH development (scale bar: 1 mm and scale bar: 50 μm). (C) Schematic diagram of intraosseous pressure (IOP) measurement in the proximal femur of rats. (D) Line chart of intraosseous pressure (IOP) changes in the proximal femur of rats during the development of ONFH.

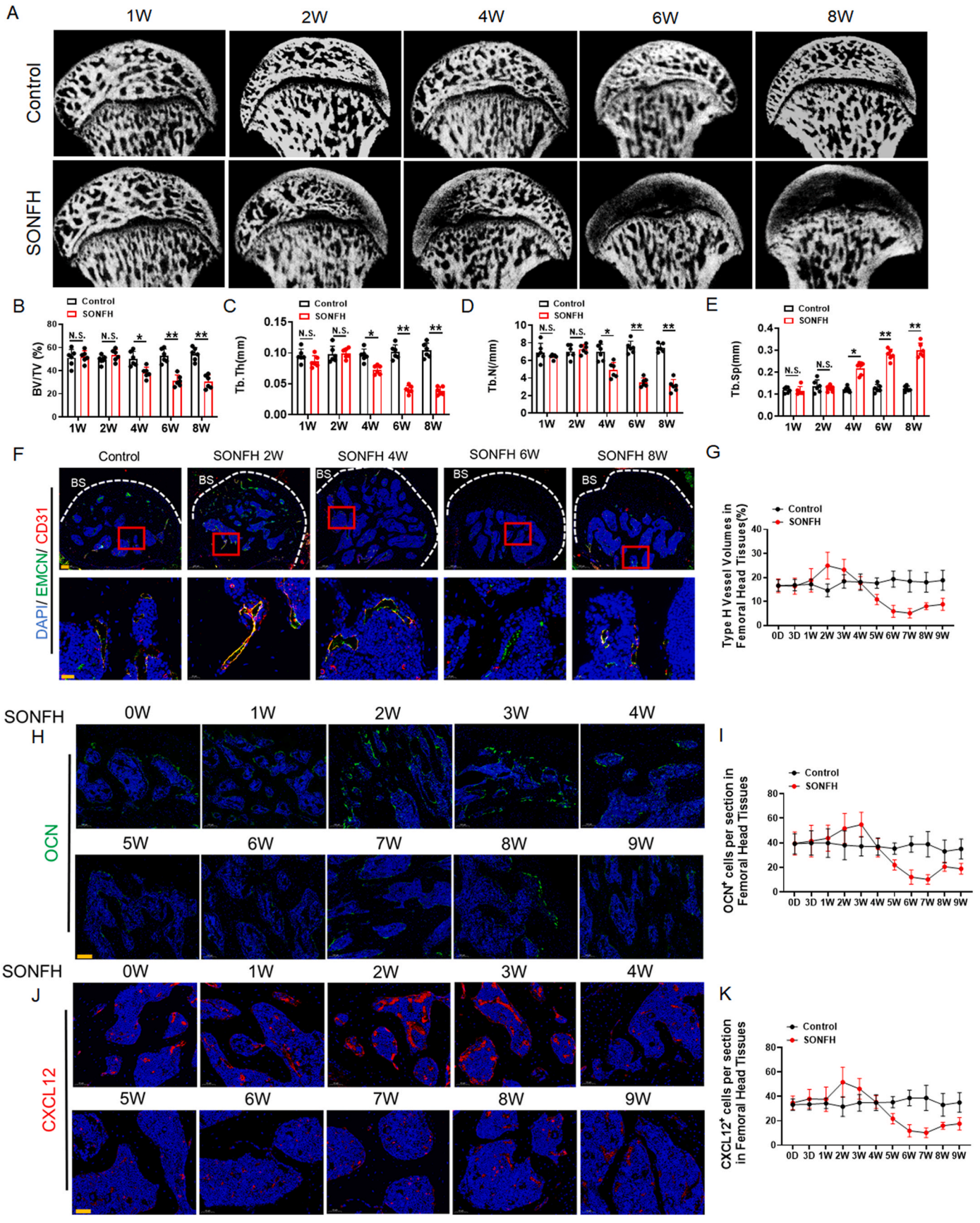

(caption on next page)

Fig. 2. Changes of bone mass, osteogenesis, and angiogenesis phenotypes in femoral head during the process of SONFH in SD rats after IOP elevation. (A) Micro-CT reconstructed images of the coronal plane of the femoral head of rats in Control and SONFH groups at 1W, 2W, 4W, 6W, and 8W. (B) Statistical analysis of femoral head bone volume fraction (BV/TV) of rats in Control and SONFH groups at 1W, 2W, 4W, 6W, and 8W. (C) Statistical analysis of trabecular bone thickness (Tb.Th) in rats in Control and SONFH groups at 1W, 2W, 4W, 6W and 8W. (D) Statistical analysis of trabecular bone number (Tb.Th) in rats in Control and SONFH groups at 1W, 2W, 4W, 6W, and 8W. (E) Statistical analysis of trabecular bone separation (Tb.Th) in rats in Control and SONFH groups at 1W, 2W, 4W, 6W and 8W. NS: No statistical difference, *P < 0.05, **P < 0.01. (F) Immunofluorescence staining was used to detect the expression changes of Type H vascular markers CD31 and EMCN in the femoral head tissue of rats in the Control and SONFH groups at 2W, 4W, 6W and 8W (scale bar: 50 μm). (G) Statistical analysis of changes in the number of Type H blood vessels in the femoral head tissue of rats in the Control and SONFH groups at 2W, 4W, 6W, and 8W after modeling. NS: No statistical difference, *P < 0.05, **P < 0.01, ***P < 0.001. (H) Immunofluorescence staining was used to detect the expression of osteogenic marker OCN in SD rat models 0D, 3D, 1W, 2W, 3W, 4W, 5W, 6W, 7W, 8W, and 9W (scale bar: 100 μm). (I) Statistical analysis of osteogenic marker OCN^+ cells at 0D, 3D, 1W, 2W, 3W, 4W, 5W, 6W, 7W, 8W and 9W of SD rat models. (J) Immunofluorescence staining was used to detect the expression of angiogenic factor CXCL12 in SD rat models 0D, 3D, 1W, 2W, 3W, 4W, 5W, 6W, 7W, 8W, and 9W (scale bar: 50 μm). (K) Statistical analysis of angiogenic marker $CXCL12^+$ cells in SD rat models at 0D, 3D, 1W, 2W, 3W, 4W, 5W, 6W, 7W, 8W and 9W.

increase from weeks 2–6, decreasing and normalizing by week 8 (Fig. 1C and D). These results indicated that in the early to mid-stage of steroid-induced osteonecrosis of the femoral head (SONFH, 2–6 weeks), intraosseous pressure increases, followed by a decrease in the later stages (6–8 weeks). In addition, based on the measurement data of H&E staining and intraosseous pressure, we found that the increase in intraosseous pressure (SONFH2W) precedes the occurrence of femoral head necrosis (SONFH4-8W).

3.2. Impact of increased intraosseous pressure in bone mass, osteogenesis, and angiogenesis phenotypes in the femoral head of SD rats

Studies have found that excess increased intraosseous pressure could lead to ONFH progression [6–8]. However, the role of moderate increased intraosseous pressure has not been elucidated yet in ONFH. In order to explore this issue, we observed the impacts of increased intraosseous pressure on bone mass, osteogenesis, and angiogenesis in the femoral head during the development of SONFH rat models. Using micro-CT scans, it was observed that the trabecular bone volume fraction (Tb. BV/TV), trabecular thickness (Tb. Th), and trabecular number (Tb. N) decreased significantly in the SONFH group compared to controls at 4, 6, and 8 weeks (Fig. 2A–E). Early-stage SONFH (2 weeks) was marked by increased intraosseous pressure and normal bone mass, with no apparent signs of osteocyte necrosis.

Immunofluorescence staining detected type H blood vessels, characterized by CD31 and EMCN markers. The SONFH 2-week group showed an increase in type H blood vessels compared to controls, which decreased significantly in later stages (4, 6, and 8 weeks) (Fig. 2F and G). This transient increase and subsequent decrease in type H vessels correlate with the progression of osteonecrosis. Osteogenesis and angiogenesis markers were examined using osteocalcin (OCN) and CXCL12. OCN-positive osteoblasts increased at 2 weeks post-MPS injection but decreased significantly after 4 weeks, continuing to decline at 6 and 8 weeks (Fig. 2H and I). Similarly, CXCL12 levels were transiently elevated early in SONFH, followed by downregulation (Fig. 2J and K). In addition, the in vitro data are consistent with the experimental results (Figs. S1A–E), jointly indicating that elevated intraosseous pressure initially promotes osteogenesis and angiogenesis but inhibits these processes in later stages, exacerbating bone vascular destruction..

3.3. Mechanosensory protein Piezo1 upregulation in response to increased intraosseous pressure

Our previous results have shown that intraosseous pressure increases in the early stage of osteonecrosis of the femoral head. However, the mechanism of increased intraosseous pressure on the femoral head has not yet been clarified. In order to explore the underlying mechanisms of increased intraosseous pressure on femoral head tissues, we collected clinical data from 10 patients with osteonecrosis of the femoral head and 10 patients with femoral neck fracture. On imaging MRI, compared with patients with femoral neck fracture, patients with ONFH showed obvious high signal in the femoral medullary cavity in T2 phase (Fig. 3A). Otherwise, histological H&E staining detection revealed that a large number of bone cells and bone marrow cells nuclei underwent karyopyknosis, and karyolysis. Recent studies have found that activation of the mechanoreceptor Piezo1 leads to the influx of calcium ions into cells and increases the expression of calcineurin in cells [27–33]. Piezo1 expression was notably upregulated among various mechanosensory proteins in response to increased intraosseous pressure (Fig. 3B). Clinical data from 10 ONFH patients and 10 femoral neck fracture patients revealed significant activation of the Piezo1 signaling pathway in ONFH patients (Table S2), evidenced by increased calcium ion influx and calcineurin expression (Fig. 3C–E). RT-PCR and Western blot analyses confirmed that Piezo1 expression was highest among mechanoreceptors (Fig. 3F–H). Immunofluorescence showed a significant increase in $Piezo1^+$ CAM^+ double-positive cells in the ONFH group (Fig. 3I and J).

Immunohistochemical staining across different modeling stages showed that Piezo1 expression increased early in SONFH (at 2 weeks), peaked with increased pressure, and decreased at the final stage (Fig. 3K–N). These results together indicated that Piezo1 might play a crucial role in the early progression of osteonecrosis of the femoral head.

3.4. Piezo1 in LEPR $^+$ bone marrow stem cell upregulates most significantly during the increased intraosseous pressure of steroid-induced osteonecrosis of the femoral head

To explore the expression changes of Piezo1 in various types of cells during the progression of osteonecrosis of the femoral head in vivo, we took femoral head specimens from rats with steroid necrosis and detected the expression changes of Piezo1 in bone marrow stem cells, endothelial cells and macrophages through histological immunofluorescence staining. Immunofluorescence staining was used to analyze Piezo1, endothelial cell marker CD31, macrophage marker CD68 and stem cell marker LEPR in the Control, SONFH 2W, and SONFH 4W groups. The expression of Piezo1/CD31 and Piezo1/LEPR fluorescent double staining suggests that compared with the Control group, the expression of Piezo1 in stem cells in the SONFH 2W group was up-regulated, and the change in endothelial Piezo1 was not obvious. However, the expression of Piezo1 in stem cells in the SONFH 4W group did not continue to be up-regulated, and endothelial Piezo1 was significantly increased at this time (Fig. 4A–D). Moreover, there is no statistical difference in the expression of Piezo1 in macrophages (Fig. 4E and F). The experimental data of this study show that in the early stage of steroid-induced necrosis of the femoral head (SONFH 2W), the signs of bone mass loss and bone cell necrosis are not obvious, indicating that the body has a physiological compensatory mechanism to resist and repair the damage caused by steroids to the femoral head. In this study, in vivo animal models found that the early increase in intraosseous pressure mainly caused the upregulation of stem cell Piezo1 expression, which may mediate osteogenesis and angiogenesis potential during the progression of early steroid-induced osteonecrosis of the femoral head and play a role in the protection of the femoral head.

In order to explore the expression of the Piezo1 signaling pathway in

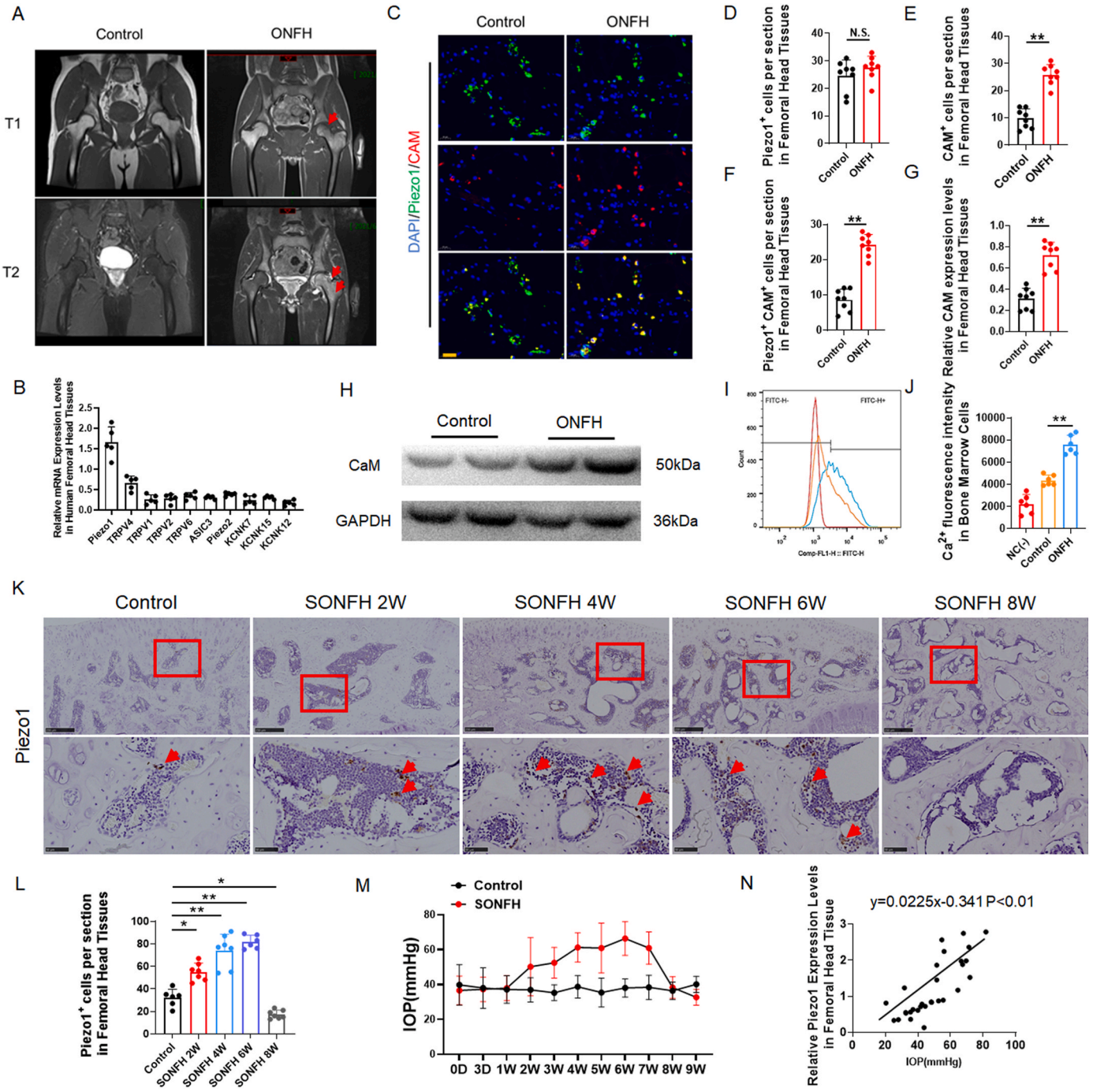

Fig. 3. Piezo1 signaling pathway expression levels in clinical specimens and animal models during IOP elevation. (A) Representative MRI images of ONFH and normal control group. (B) Relative expression levels of mechanoreceptor gene mRNA in human femoral head tissue. (C) Immunofluorescence staining in Control and ONFH groups shows the expression of Piezo1 protein and CAM protein in femoral head tissues (scale bar: 20 μm). (D–F) Statistical analysis of $Piezo1^{+}$, CAM^{+} and $Piezo1^{+}CAM^{+}$ cells in Control and ONFH groups. (G) Relative expression levels of CAM protein in Control and ONFH groups. (H) Statistical analysis of CAM protein expression in Control and ONFH groups. (I–J) Ca^{2+} inflorescence intensity in bone marrow cells of Control and ONFH groups. (K) Immunohistochemical staining of Control, SONFH 2W, SONFH 4W, SONFH 6W, and SONFH 8W groups shows Piezo1 protein expression in femoral head tissue (scale bar: 250 μm and scale bar: 50 μm). (L) Statistical analysis of $Piezo1^{+}$ cells in Control, SONFH 2W, SONFH 4W, SONFH 6W, and SONFH 8W groups. (M) IOP measurement in the proximal femur of rats from SONFH 0W to SONFH 9W. (N) Relative Piezo1 expression in femoral head tissues with the IOP elevation. NS: No statistical difference, *P < 0.05, **P < 0.01.

various cells in the bone marrow cavity in response to mechanical stimulation, this study examined BMSCs (bone marrow mesenchymal stem cells), ECs (endothelial cells), OBs (osteoblasts), and Mφ (macrophages) were subjected to pressurization treatment, while the cells in the control group were not pressurized. Immunofluorescence staining was used to detect the intensity of calcium ion influx (Fluo 4) in BMSC, EC, OB, and Mφ under mechanical stimulation conditions. The results showed that there were significant changes in calcium ion influx in BMSC, EC, and OB cells. However, the calcium ion influx in BMSCs increased most significantly than others (Figs. S2A-B). RT-PCR detection of Piezo1 mRNA expression in BMSC, EC, OB, and Mφ under mechanical stimulation conditions also showed that the expression of Piezo1

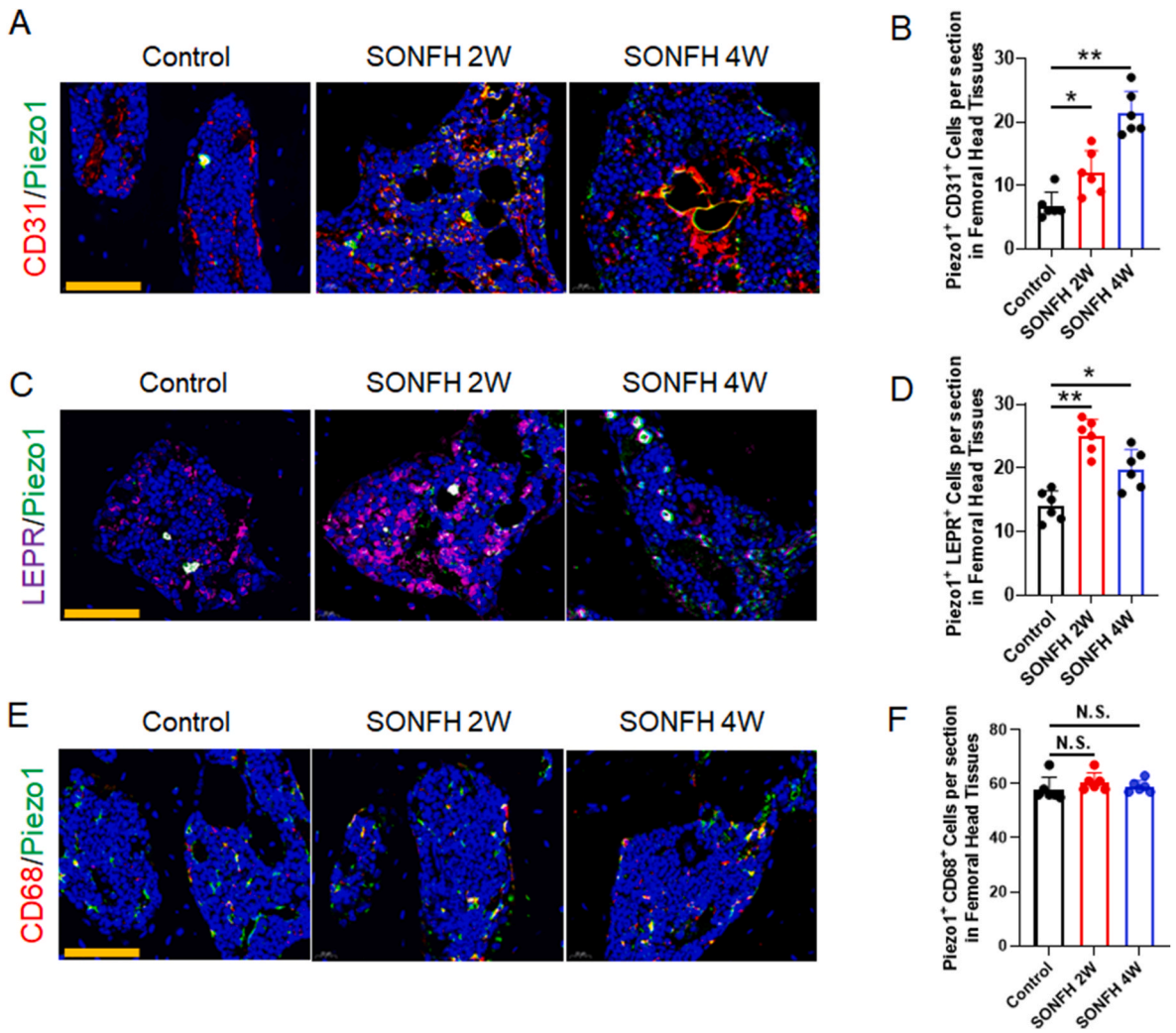

Fig. 4. Piezo1 in LEPR $^{+}$ bone marrow stem cell upregulates most significantly during IOP changes in SONFH rats. (A, C, and E) Double fluorescent staining of Piezo1/CD31, Piezo1/LEPR and Piezo1/CD68 in Control, SONFH 2W, and SONFH 4W groups (scale bar: 40 μm). (B, D, and F) Statistical analysis of Piezo1/CD31 expression in Control, SONFH 2W, and SONFH 4W groups. (F) Statistical analysis of Piezo1/LEPR expression in Control, SONFH 2W, and SONFH 4W groups. NS: No statistical difference, *P < 0.05, **P < 0.01.

increased most significantly in mesenchymal stem cells (Fig. S2C). In conclusion, various cells in the bone marrow produce different effects in response to mechanical stimulation. In vitro experiments, bone marrow mesenchymal stem cells respond most obviously to mechanical stimulation.

3.5. Inhibition of stem cell Piezo1 by GsMTx4 promotes the increase in intraosseous pressure and aggravates the progression of osteonecrosis of the femoral head

According to the above experimental results, it can be seen that the early increase in intraosseous pressure during the modeling process of osteonecrosis of the femoral head mainly upregulates stem cell Piezo1. In order to explore whether early targeted inhibition of stem cell Piezo1 can affect the progression of osteonecrosis of the femoral head, we injected the Piezo1 small molecule inhibitor GsMTX4 into rats to inhibit the Piezo1 signaling pathway, and continued to inject steroids to establish an osteonecrosis of the femoral head model (Fig. 5A). The results showed that after administration of GsMTx4, the increase in intraosseous pressure aggravated in SONFH 4W group, and the degree of osteonecrosis of the femoral head in the HE staining was more severe than that in the ordinary model group (Fig. 5B–E). The changes in bone mass in the late stages of necrosis modeling after GsMTX4 administration were further examined. Micro-CT results showed that early inhibition of Piezo1 could significantly aggravate the bone mass loss caused by necrosis modeling (Fig. 5F–I). In addition, immunofluorescence staining results suggest that GsMTx4 inhibits the osteogenic and angiogenic functions (indicated by OCN, CD31/EMCN, and CXCL12 expression levels) of stem cells by inhibiting the NFAT1 signaling pathway (Fig. 5K–O). The above experimental results collectively indicate that early inhibition of stem cell Piezo1 by injection of GsMTx4 can aggravate the increase in intraosseous pressure and aggravate the process of osteonecrosis of the femoral head.

3.6. Piezo1 activation regulates the osteogenic and angiogenic potential of stem cells through the CAM-NFAT1 signaling pathway

Studies have found that mechanical stimulation can mediate the NFAT1 signaling pathway in mesenchymal stem cells to promote osteogenesis and angiogenesis in the body [48,49]. In order to further verify how Piezo1 works after activation in vivo, this study injected Yoda1 into rats and verified the femoral head tissue specimens. In order to further elucidate how Piezo1 functions after activation in femoral head tissues, we injected Yoda1 into rats to activate the Piezo1 signaling pathway. Immunofluorescence staining of the Control and Yoda1 groups showed the expression of OCN, CD31/Emcn, and LEPR/NFAT1 in the

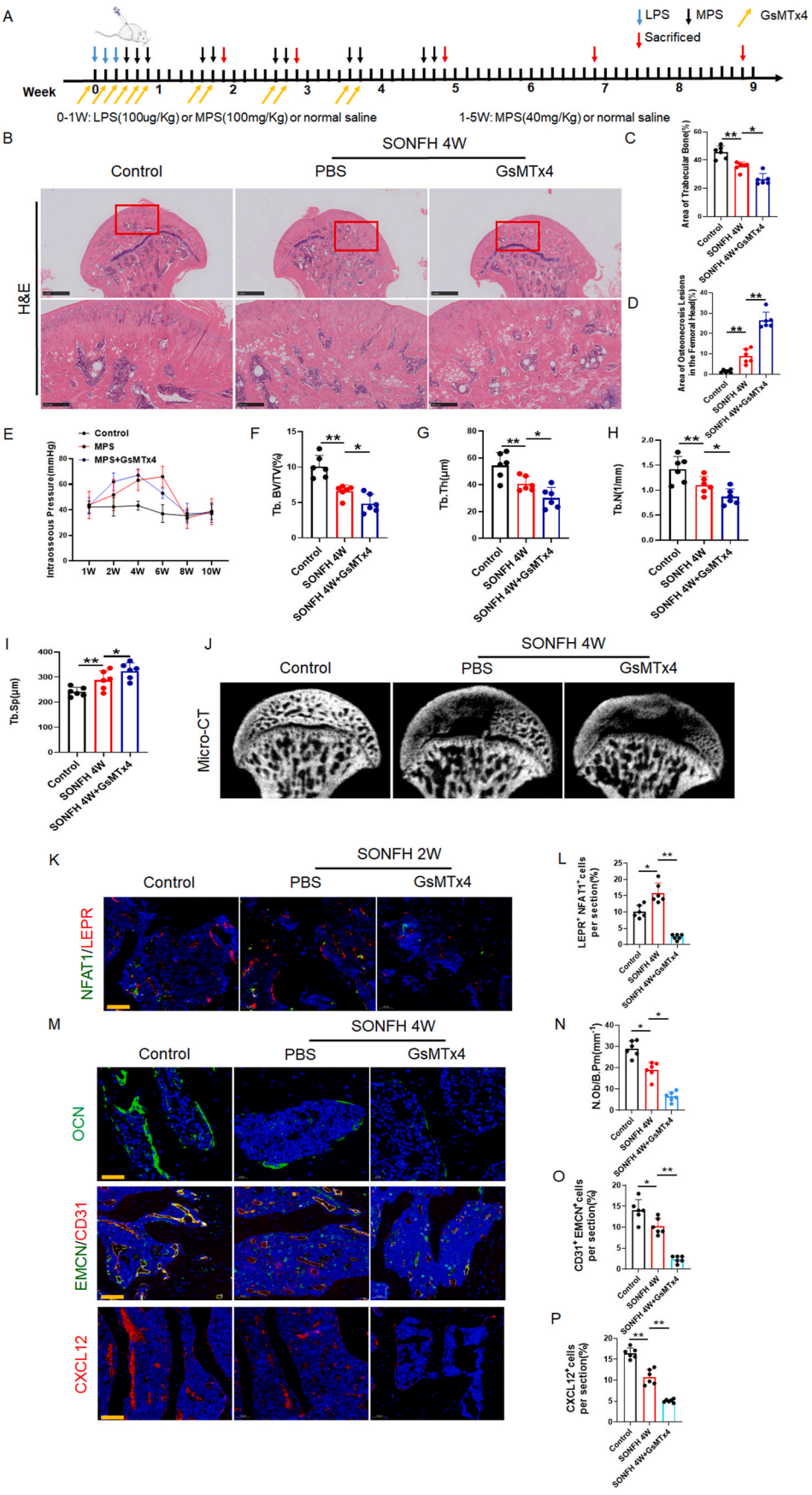

(caption on next page)

Fig. 5. Inhibition of stem cell Piezo1 by GsMTx4 promotes the increase in intraosseous pressure and aggravates the progression of SONFH. (A) Schematic diagram of SD rat's models. (B) HE changes in femoral head tissue in SD rats in PBS, MPS, and GsMTx4-MPS groups 4 weeks after modeling (scale bar: 1 mm and scale bar: 50 μm). (C) Statistical analysis of area of trabecular bone (%). (D) Statistical analysis of area of osteonecrosis lesions in the femoral head (%). (E) IOP measurement in rat proximal femur. (F) Statistical analysis of femoral head bone volume fraction (BV/TV) of SD rats in PBS, MPS, and GsMTx4-MPS groups 4 weeks after modeling. (G) Statistical analysis of femoral head trabecular bone thickness (Tb.Th) in SD rats in PBS, MPS, and GsMTx4-MPS groups 4 weeks after modeling. (H) Statistical analysis of trabecular bone number (Tb.N) in the femoral head of SD rats in PBS, MPS, and GsMTx4-MPS groups 4 weeks after modeling. (I) Statistical analysis of femoral head trabecular separation (Tb.Sp) in SD rats in PBS, MPS, and GsMTx4-MPS groups 4 weeks after modeling. NS: No statistical difference, *P < 0.05, **P < 0.01, P***<0.001. (J) Micro-CT reconstructed images of the coronal plane of the femoral head in SD rats in the PBS, MPS, and GsMTx4-MPS groups 4 weeks after modeling. (K) Immunofluorescence staining of NFAT1/LEPR in the femoral head tissues of SD rats from the PBS, MPS, and GsMTx4-MPS groups 4 weeks post-modeling (scale bar: 50 um). (L) Statistical analysis of changes in NFAT1/LEPR expression in the femoral head tissues of SD rats from the PBS, MPS, and GsMTx4-MPS groups 4 weeks post-modeling. (M) Immunofluorescence staining of OCN, CD31/EMCN, and CXCL12 in the femoral head tissues of SD rats from the PBS, MPS, and GsMTx4-MPS groups 4 weeks post-modeling (scale bar: 20 um and scale bar: 50 um). (O–P) Statistical analysis of changes in OCN, CD31/EMCN, and CXCL12 expression in the femoral head tissues of SD rats from the PBS, MPS, and GsMTx4-MPS groups 4 weeks post-modeling. N.S.: No statistical difference, *P < 0.05, **P < 0.01, ***P < 0.001.

femoral head tissues. Results showed that the expression of NFAT1 in stem cells was up-regulated, and this effect could be inhibited by targeting calcium ions with KN93 (Fig. 6A–F). These indicated that in vivo activation of Piezo1 could regulate the osteogenic and angiogenic potential of stem cells via CAM-NFAT1 signaling pathways.

In addition, in vitro experiments also showed that activating Piezo1 could promote calcium influx in stem cells and promote endothelial tube formation after co-culture with endothelial cells. This effect could be inhibited by targeting calcium ions with KN93 (Fig. 6G–I). The expression of VEGFA and RUNX2 genes detected by Western blotting, Ca^{2+} imaging, and double immunofluorescence staining of RUNX2/CXCL12 also confirmed the above results (Fig. 6J–P). These results indicated that inhibiting NFAT1 can weaken the promotion effect of Yoda1 on stem cell osteogenesis and angiogenesis, and inhibiting NFAT1 has no effect on intracellular calcium influx.

4. Discussion

Studies have found that most ONFH have a common pathological process: tissue ischemia and bone cell apoptosis or necrosis, which are accompanied by increased lipogenesis and vascular obstruction, leading to a sharp increase in the pressure in the medullary cavity of the femoral head, which in turn leads to the ischemia of the femoral head [10]. A large number of studies have shown that intraosseous pressure increases in patients with osteonecrosis of the femoral head secondary to high doses of glucocorticoids or excess alcohol [11]. Some clinical studies have proven that performing core decompression surgery to reduce intraosseous pressure in the early stage of osteonecrosis of the femoral head could prevent or slow down its evolution, which has significant clinical significance [12].

There is a close relationship between the temporal changes in intraosseous pressure and the pathogenesis and repair difficulties of femoral head necrosis. The increase in intraosseous pressure may lead to insufficient blood supply and bone cell damage, while the decrease in intraosseous pressure may affect the healing ability of bone tissue. Therefore, monitoring and regulating intraosseous pressure is of great significance in the prevention and treatment of femoral head necrosis. Interventions targeting changes in intraosseous pressure, such as improving blood supply and promoting bone tissue regeneration, may help improve the prognosis of patients with femoral head necrosis [11–14]. After the intraosseous venous return disorder produces intraosseous high pressure, it can lead to the formation of new bone around the necrotic area of the femoral head, inducing various pathological changes such as osteosclerosis and osteoarthritis. Under intraosseous high pressure, the rheological state of systemic blood and local bone marrow is obviously abnormal, and local blood circulation in the femoral head tissue is disrupted [14,15].

Based on this, this study established a rat model of steroid-induced osteonecrosis of the femoral head and collected specimens from clinical patients with osteonecrosis of the femoral head. Then we examined the changes in intraosseous pressure over time during the modeling process of steroid-induced osteonecrosis, as well as the changes in femoral head phenotypes after the increase in intraosseous pressure. At the same time, since the increase in pressure mainly exerts its effect through changes in the mechanoreceptor Piezo1 and downstream calcium ion influx, after the intraosseous pressure increases, this study detected calcium ion influx and downstream key signaling pathway proteins, such as NFAT signaling, BMP signaling and other signaling pathway key proteins, clarifying the signaling pathways and key mechanisms responsible for the increase in intraosseous pressure.

Piezo1 is a new type of mechanoreceptor, expressed in many organs throughout the body and was discovered by Patapoutian, the 2021 Nobel Prize winner. Under physiological conditions, osteoblast Piezo1 maintains bone homeostasis by responding to mechanical stimulation [15–17,20,21]. Studies have found that vascular endothelium can also regulate vascular endothelial homeostasis in response to mechanical stimulation through Piezo1, a molecular switch of calcium ion channels [24]. In addition, endothelial-specific expression of Piezo1 plays an important role in angiogenesis, regulating endothelial osmotic pressure, and blood pressure homeostasis. Moderate exercise activates Piezo1 to increase H-type angiogenesis and the number of capillaries, prevent the apoptosis of skeletal muscle endothelial cells, and prevent microvascular from loosening [22]. Under pathological conditions, Piezo1 in the endothelium of small pulmonary blood vessels senses blood pressure changes and regulates endothelial stretching and osmotic pressure, leading to pulmonary edema. In disease models of diabetes and hyperlipidemia, excessive activation of Piezo1 expression in the vascular endothelium can cause endothelial cell dysfunction and lead to microvascular thrombosis. Inhibition of Piezo1 expression can significantly improve the damage to microvascular homeostasis [43,44]. This study found that during the progression of steroid-induced osteonecrosis of the femoral head, intraosseous pressure continues to increase. In the early stage of animal modeling (SONFH 2W), stem cell Piezo1 is mainly activated, mediates osteogenesis and vascularization, and exerts negative feedback on hormonal damage in the body, thus playing a repair effect. Otherwise, Piezo1 is used to early promote the osteogenic and vascular potential of stem cells, which could curb further increases in pressure, improve the damaging effects of hormones on stem cells and blood vessels, and help to alleviate early treatment of osteonecrosis of the femoral head.

This study also has some limitations, such as the specific mechanism of increased intraosseous pressure that needs further exploration. Factors affecting intraosseous pressure mainly include blood vessel destruction and accumulation of fat in the bone marrow. More experimental evidence is needed to explain how hormones cause an increase in intraosseous pressure in the body.

In summary, this study explored the changes in intraosseous pressure during the progression of steroid-induced osteonecrosis of the femoral head and the changes in signaling pathways produced by mechanoreceptors in bone marrow cells in response to changes in intraosseous pressure. we clarified that the intraosseous pressure increases in the early to middle-stage (increase at 2–6W) during the modeling process of

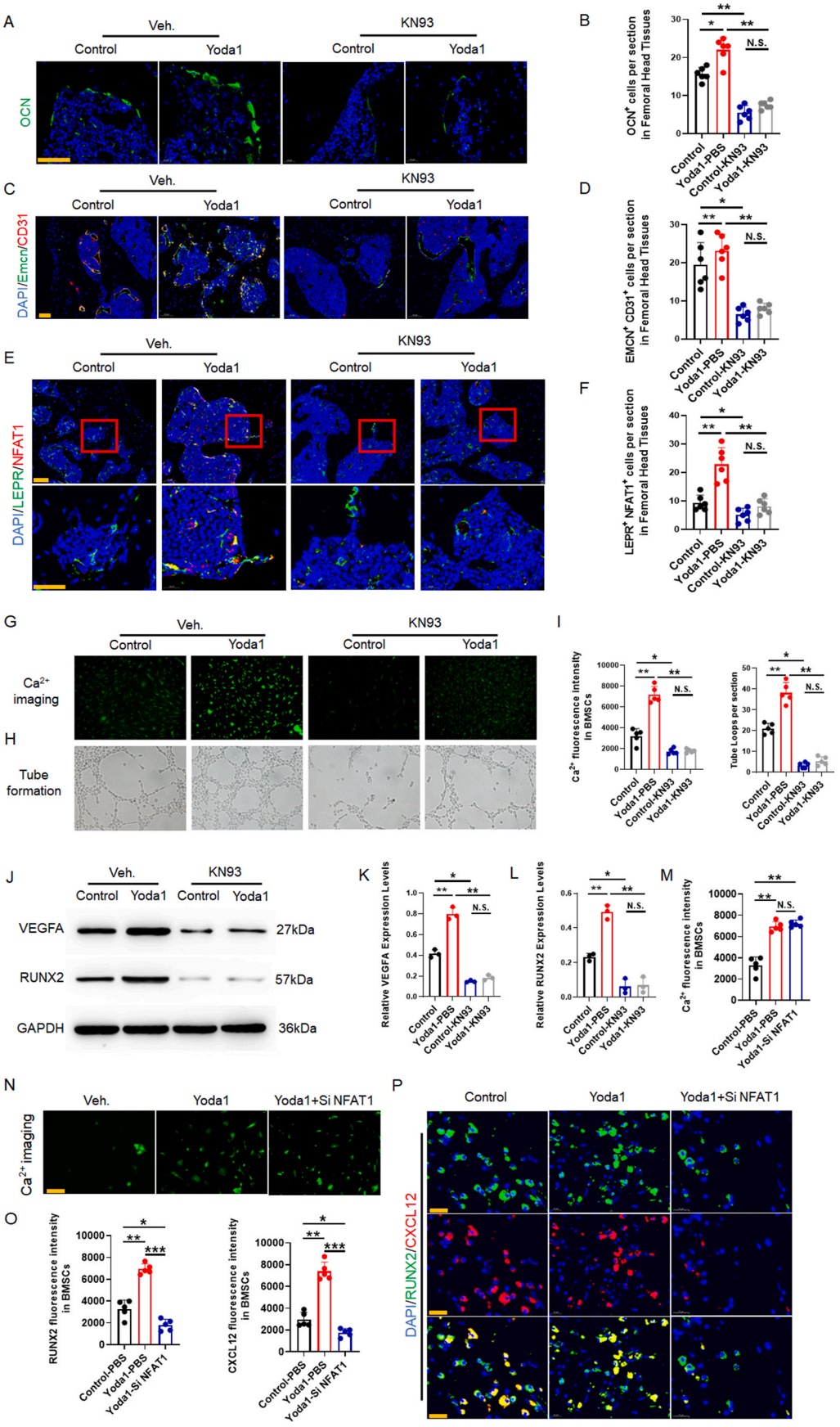

(caption on next page)

Fig. 6. Piezo1 regulates the osteogenic and angiogenic potential of BMSCs through the CAM-NFAT1 signaling pathway. (A–B) Immunofluorescence staining of OCN expression in femoral head tissues of the Control and Yoda1 groups, veh, and KN93 treated groups along with statistical analysis (scale bar: 40 μm). (C–D) Immunofluorescence staining of CD31 and Emcn expression in femoral head tissues of the Control and Yoda1 groups, veh, and KN93 treated groups along with statistical analysis (scale bar: 40 μm). (E–F) Immunofluorescence staining of LEPR and NFAT1 expression in femoral head tissues of the Control and Yoda1 groups, veh, and KN93 treated groups along with statistical analysis (scale bar: 40 μm). (G) Ca^{2+} imaging in BMSCs of the Control and Yoda1 groups, veh, and KN93 treated groups. (H) Tube formation analysis in ECs co-culture with BMSCs of SD rat models of the Control and Yoda1 groups, veh, and KN93 treated groups. (I) Statistical analysis of relative expression of Ca^{2+} intensity and tube loops of Control and Yoda1 groups, veh, and KN93 treated groups. (J) Protein expression of NFAT1, VEGFA, and RUNX2 in the Control and Yoda1 groups. (K–L) Statistical analysis of relative expression of VEGFA and RUNX2 proteins in the Control and Yoda1 groups, veh, and KN93 treated groups. (M−N) Ca^{2+} imaging and statistical analysis of relative expression of Ca^{2+} intensity in BMSCs of the Control Yoda1 and Yoda1+Si NFAT1 groups. (O–P) Immunofluorescence staining of RUNX2 and CXCL12 expression in BMSCs of the Control Yoda1 and Yoda1+Si NFAT1 groups along with statistical analysis (scale bar: 20 μm). N.S.: No statistical difference, *P < 0.05, **P < 0.01, ***P < 0.001.

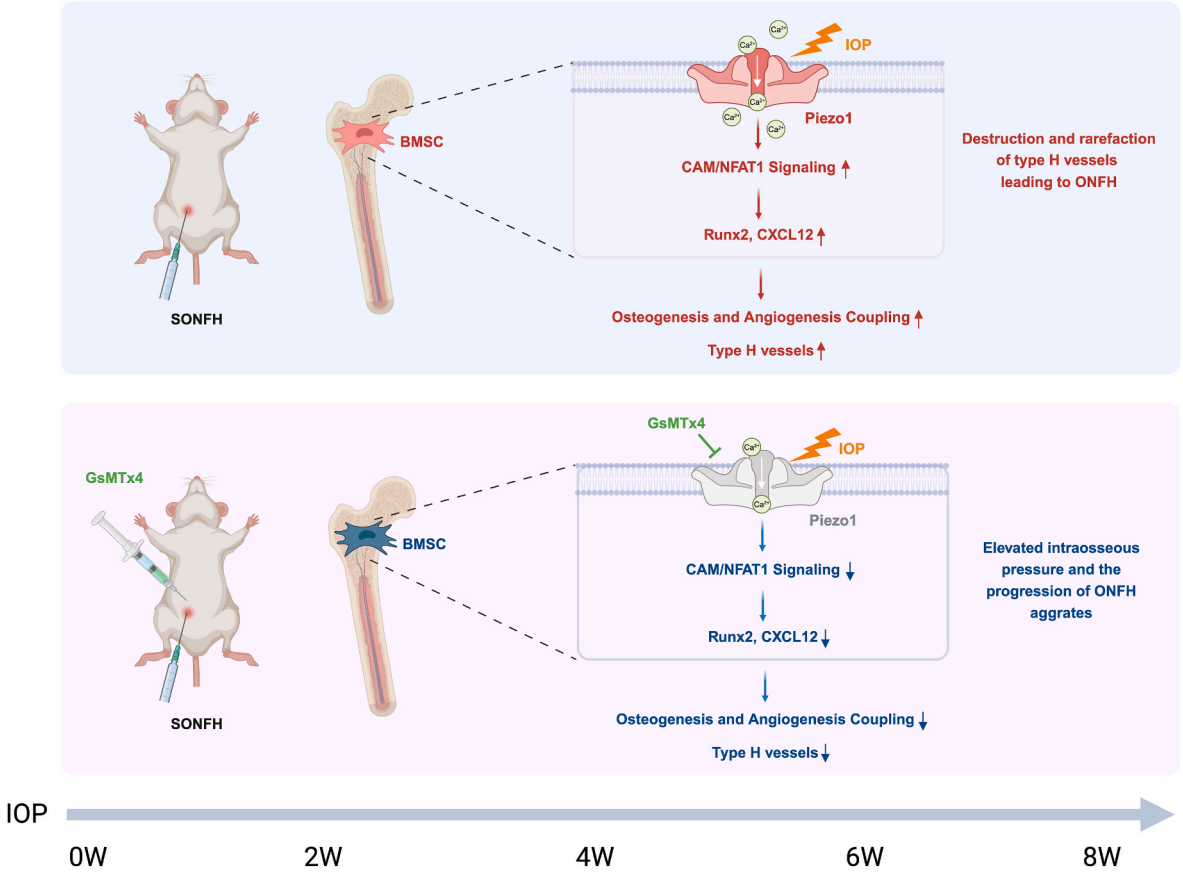

Fig. 7. A model of SONFH reveals that BMSC Piezo1 in response to elevated IOP regulates bone vascular homeostasis through CAM-NFAT1 signaling pathway. (A) During the development of SONFH, Piezo1 can respond to the increased intraosseous pressure and promote the osteogenesis and vascular potential of bone marrow mesenchymal stem cells through the CAM-NFAT1 signaling pathway in the early stage. (B) Early inhibition of stem cell Piezo1 by injection of GsMTx4 can aggravate the increase in intraosseous pressure and the progression of SONFH through Piezo1-CAM-NFAT1 signaling pathway. Created in https://BioRender.com.

SD rats, and does not increase but decreases in the late stage (6–8W), resulting in the destruction and rarefaction of femoral head bone mass and blood vessels, which is responsible for the key cause of osteonecrosis of the femoral head. In order to solve these problems, more basic experimental research is needed to explore. Furthermore, Piezo1 can regulate the osteogenic and angiogenic potential of bone marrow mesenchymal stem cells in response to increased intraosseous pressure, and plays an important role in the progression of osteonecrosis of the femoral head. Targeting Piezo1 to early promote the osteogenic and vascular potential of stem cells, which could curb further increases in pressure, improve the damaging effects of glucocorticoids on stem cells and blood vessels, and contribute to early treatment of osteonecrosis of the femoral head. Finally, scientific research should serve clinical practice and relieve patients' symptom. Currently, many mechanisms of the impact of elevated intraosseous pressure on osteonecrosis of the femoral head are still in the basic theoretical research stage, and we hope to translate them into clinical applications as soon as possible.

5. Conclusion

This study demonstrates that steroid-induced ONFH mediates a sustained increase in intraosseous pressure, initially promoting osteogenesis and angiogenesis, which are later inhibited. Mechanistically, increased intraosseous pressure upregulates the Piezo1 signaling pathway in bone marrow stem cells, enhancing CXCL12 secretion through the CAM-NFAT1 signaling pathway early in the disease. Consequently, Piezo1 plays a protective role in early-stage osteonecrosis but contributes to vascular damage and disease progression when pressure is excessively increased (Fig. 7).

Declaration of competing interest

The authors have no conflicts of interest to disclose in relation to this article.

Acknowledgement

This work was supported by the National Natural Science Foundation of China (No. 82472439, No. 82270935, No. 81974337, No. 81672155) and the Key Projects of Natural Science Research in Colleges and Universities in Anhui Province (Grant No. 2024AH051263 and 2022AH051444).

Appendix A. Supplementary data

Supplementary data to this article can be found online at https://doi.org/10.1016/j.jot.2025.01.008.

References

[1] Cohen-Rosenblum A, Cui Q. Osteonecrosis of the femoral head. Orthop Clin N Am 2019;50(2):139–49.
[2] Khosla S, Wright NC, Elderkin AL, Kiel DP. Osteoporosis in the USA: prevention and unmet needs. Lancet Diabetes Endocrinol 2023;11(1):19–20.
[3] Li Z, Shao W, Lv X, Wang B, Han L, Gong S, et al. Advances in experimental models of osteonecrosis of the femoral head. Journal of Orthopaedic Translation 2023;39:88–99.
[4] Shao W, Li Z, Wang B, Gong S, Wang P, Song B, et al. Dimethyloxalylglycine attenuates steroid-associated endothelial progenitor cell impairment and osteonecrosis of the femoral head by regulating the HIF-1α signaling pathway. Biomedicines 2023;11(4):992.
[5] Hoogervorst P, Campbell JC, Scholz N, Cheng EY. Core decompression and bone marrow aspiration concentrate grafting for osteonecrosis of the femoral head. J Bone Joint Surg 2022;104(Suppl 2):54–60.
[6] Quinlan ND, Chen DQ, Werner BC, Cui Q. Outcomes following total hip arthroplasty for femoral head osteonecrosis in patients with history of solid organ transplant. J Bone Joint Surg 2022;104(Suppl 2):76–83.
[7] Lou P, Zhou G, Wei B, Deng X, Hou D. Bone grafting for osteonecrosis of the femoral head in the past decade: a systematic review and network meta-analysis. Int J Surg 2023;109(3):412–8.
[8] Divi SN, Bielski RJ. Legg-calve-perthes disease. Pediatr Ann 2016;45(4):e144–9.
[9] Larson E, Jones LC, Goodman SB, Koo KH, Cui Q. Early-stage osteonecrosis of the femoral head: where are we and where are we going in year 2018? Int Orthop 2018;42(7):1723–8.
[10] Arbab D, König DP. Atraumatic femoral head necrosis in adults. Deutsches Arzteblatt International 2016;113(3):31–8.
[11] Mukisi MM, Bashoun K, Burny F. Sickle-cell hip necrosis and intraosseous pressure. Orthopaedics & traumatology, surgery & research: OTSR 2009;95(2):134–8.
[12] Elder GJ. From marrow oedema to osteonecrosis: common paths in the development of post-transplant bone pain. Nephrology 2006;11(6):560–7.
[13] Uchio Y, Ochi M, Adachi N, Nishikori T, Kawasaki K. Intraosseous hypertension and venous congestion in osteonecrosis of the knee. Clin Orthop Relat Res 2001;384:217–23.
[14] Lee MS, Hsieh PH, Chang YH, Chan YS, Agrawal S, Ueng SW. Elevated intraosseous pressure in the intertrochanteric region is associated with poorer results in osteonecrosis of the femoral head treated by multiple drilling. J Bone Joint Surg 2008;90(7):852–7.
[15] Lin YC, Guo YR, Miyagi A, Levring J, MacKinnon R, Scheuring S. Force-induced conformational changes in PIEZO1. Nature 2019;573(7773):230–4.
[16] Hill RZ, Loud MC, Dubin AE, Peet B, Patapoutian A. PIEZO1 transduces mechanical itch in mice. Nature 2022;607(7917):104–10.
[17] Coste B, Mathur J, Schmidt M, Earley TJ, Ranade S, Petrus MJ, et al. Piezo1 and Piezo2 are essential components of distinct mechanically activated cation channels. Science 2010;330(6000):55–60.
[18] Lim GB. Piezo1 senses pressure overload and initiates cardiac hypertrophy. Nat Rev Cardiol 2022;19(8):503.
[19] Sun M, Mao S, Wu C, Zhao X, Guo C, Hu J, et al. Piezo1-Mediated neurogenic inflammatory cascade exacerbates ventricular remodeling after myocardial infarction. Circulation 2024 Jan 18.
[20] Chen S, Li Z, Chen D, Cui H, Wang J, Li Z, et al. Piezo1-mediated mechanotransduction promotes entheseal pathological new bone formation in ankylosing spondylitis. Ann Rheum Dis 2023;82(4):533–45.
[21] Wang L, You X, Lotinun S, Zhang L, Wu N, Zou W, et al. Mechanical sensing protein PIEZO1 regulates bone homeostasis via osteoblast-osteoclast crosstalk. Nat Commun 2020;11(1):282.
[22] Bartoli F, Debant M, Chuntharpursat-Bon E, Evans EL, Musialowski KE, Parsonage G, et al. Endothelial Piezo1 sustains muscle capillary density and contributes to physical activity. J Clin Investig 2022:e141775.
[23] Sugimoto A, Miyazaki A, Kawarabayashi K, Shono M, Akazawa Y, Hasegawa T, et al. Piezo type mechanosensitive ion channel component 1 functions as a regulator of the cell fate determination of mesenchymal stem cells. Sci Rep 2017;7(1):17696. 18.
[24] Qin L, He T, Chen S, Yang D, Yi W, Cao H, et al. Roles of mechanosensitive channel Piezo1/2 proteins in skeleton and other tissues. Bone Research 2021;20(1):44. 9.
[25] Steward AJ, Kelly DJ. Mechanical regulation of mesenchymal stem cell differentiation. J Anat 2015;227(6):717–31.
[26] Liu Y, Tian H, Hu Y, Cao Y, Song H, Lan S, et al. Mechanosensitive Piezo1 is crucial for periosteal stem cell-mediated fracture healing. Int J Biol Sci 2022;13(10):3961–80. 18.
[27] Sasaki F, Hayashi M, Mouri Y, Nakamura S, Adachi T, Nakashima T. Mechanotransduction via the Piezo1-Akt pathway underlies Sost suppression in osteocytes. Biochem Biophys Res Commun 2020;521(3):806–13.
[28] Zhang X, Hou L, Li F, Zhang W, Wu C, Xiang L. Piezo1-mediated mechanosensation in bone marrow macrophages promotes vascular niche regeneration after irradiation injury. Theranostics 2022;12(4):1621–38.
[29] Lee W, Nims RJ, Savadipour A, Zhang Q, Leddy HA, Liu F, et al. Inflammatory signaling sensitizes Piezo1 mechanotransduction in articular chondrocytes as a pathogenic feed-forward mechanism in osteoarthritis. Proc Natl Acad Sci USA 2021;118(13):e2001611118.
[30] Friedrich EE, Hong Z, Xiong S, Zhong M, Di A, Rehman J, et al. Endothelial cell Piezo1 mediates pressure-induced lung vascular hyperpermeability via disruption of adherens junctions. Proc Natl Acad Sci USA 2019;116(26):12980–5.
[31] Sun Y, Leng P, Song M, Li D, Guo P, Xu X, et al. Piezo1 activates the NLRP3 inflammasome in nucleus pulposus cell-mediated by Ca^{2+}/NF-κB pathway. Int Immunopharm 2020;85:106681.
[32] Hines JT, Jo WL, Cui Q, Mont MA, Koo KH, Cheng EY, et al. Osteonecrosis of the femoral head: an updated review of ARCO on pathogenesis, staging and treatment. J Kor Med Sci 2021;36(24):e177.
[33] Weinstein RS. Glucocorticoid-induced osteonecrosis. Endocrine 2012;41(2):183–90.
[34] Zheng Y, Zheng Z, Zhang K, Zhu P. Osteonecrosis in systemic lupus erythematosus: systematic insight from the epidemiology, pathogenesis, diagnosis and management. Autoimmun Rev 2022;21(2):102992.
[35] Chen Y, Miao Y, Liu K, Xue F, Zhu B, Zhang C. Evolutionary course of the femoral head osteonecrosis: histopathological - radiologic characteristics and clinical staging systems. Journal of Orthopaedic Translation 2021;32:28–40.
[36] Quan H, Ren C, He Y, Wang F, Dong S, Jiang H. Application of biomaterials in treating early osteonecrosis of the femoral head: research progress and future perspectives. Acta Biomater 2023;164:15–73.
[37] Meng K, Liu Y, Ruan L, Chen L, Chen Y, Liang Y. Suppression of apoptosis in osteocytes, the potential way of natural medicine in the treatment of osteonecrosis of the femoral head. Biomed Pharmacother 2023;162:114403.
[38] Li R, Lin QX, Liang XZ, Liu GB, Tang H, Wang Y. Stem cell therapy for treating osteonecrosis of the femoral head: from clinical applications to related basic research. Stem Cell Res Ther 2018;9(1):291.
[39] Chang C, Greenspan A, Gershwin ME. Gershwin. The pathogenesis, diagnosis and clinical manifestations of steroid-induced osteonecrosis. J Autoimmun 2020;110:102460.
[40] Rackwitz L, Eden L, Reppenhagen S, Reichert JC, Jakob F, Walles H. Stem cell- and growth factor-based regenerative therapies for avascular necrosis of the femoral head. Stem Cell Res Ther 2012 Feb 22;3(1):7.
[41] Xu H, Wang C, Liu C, Peng Z, Li J, Jin Y, et al. Cotransplantation of mesenchymal stem cells and endothelial progenitor cells for treating steroid-induced osteonecrosis of the femoral head. Stem Cells Translational Medicine 2021;10(5):781–96.
[42] Maruyama M, Pan CC, Moeinzadeh S, Storaci HW, Guzman RA, Lui E, et al. Effect of porosity of a functionally-graded scaffold for the treatment of corticosteroid-associated osteonecrosis of the femoral head in rabbits. Journal of Orthopaedic Translation 2021;28:90–9.
[43] Hoogervorst P, Campbell JC, Scholz N, Cheng EY. Core decompression and bone marrow aspiration concentrate grafting for osteonecrosis of the femoral head. J Bone Jt Surg Am Vol 2022;104(Suppl 2):54–60.
[44] Andronic O, Hincapié CA, Burkhard MD, Loucas R, Loucas M, Ried E, et al. Lack of conclusive evidence of the benefit of biologic augmentation in core decompression for nontraumatic osteonecrosis of the femoral head: a systematic review. Arthroscopy 2021;37(12):3537–3551.e3.
[45] Engelmayr GC Jr, Sales VL, Mayer Jr JE, Sacks MS. Cyclic flexure and laminar flow synergistically accelerate mesenchymal stem cell-mediated engineered tissue formation: implications for engineered heart valve tissues. Biomaterials 2006 Dec;27(36):6083–95.
[46] Huang Y, Jia X, Bai K, Gong X, Fan Y. Effect of fluid shear stress on cardiomyogenic differentiation of rat bone marrow mesenchymal stem cells. Arch Med Res 2010 Oct;41(7):497–505.
[47] Ye X, Zhao Q, Sun X, Li H. Enhancement of mesenchymal stem cell attachment to decellularized porcine aortic valve scaffold by in vitro coating with antibody against CD90: a preliminary study on antibody-modified tissue-engineered heart valve. Tissue Eng 2009 Jan;15(1):1–11.
[48] Kong L, Zuo R, Wang M, Wang W, Xu J, Chai Y, et al. Silencing MicroRNA-137-3p, which targets RUNX2 and CXCL12 prevents steroid-induced osteonecrosis of the femoral head by facilitating osteogenesis and angiogenesis. Int J Biol Sci 2020 Jan 14;16(4):655–70.
[49] Yang T, Zhang J, Cao Y, Zhang M, Jing L, Jiao K, et al. Wnt5a/Ror2 mediates temporomandibular joint subchondral bone remodeling. J Dent Res 2015 Jun;94(6):803–12.